



Bamboo node effect on the tensile properties of side press-laminated bamboo lumber

Zhen Wang^{1,2} · Haitao Li^{1,2} · Dong Yang^{1,2} · Zhenhua Xiong³ · Usama Sayed^{1,2} · Rodolfo Lorenzo⁴ · Ileana Corbi⁵ · Ottavia Corbi⁵ · Chaokun Hong^{1,2}

Received: 18 April 2020 / Accepted: 30 November 2020 / Published online: 4 January 2021
© The Author(s), under exclusive licence to Springer-Verlag GmbH, DE part of Springer Nature 2021

Abstract

At present, most of the existing studies on bamboo nodes focus on the raw bamboo. There is still a lack of researches on the nodes in side press-laminated bamboo lumber (LBL). However, after processing, bamboo nodes in the laminated bamboo lumber are different from the raw bamboo nodes in terms of performance. Therefore, this paper carried out tests to analyze the influence of bamboo node on the tensile properties parallel to grain of side press-laminated bamboo lumber. A total of 180 specimens were divided into six groups, and the number and position of the bamboo nodes at the specimen in each group were different. The effects of these factors on the strength, elastic modulus, and Poisson's ratio of the side press-laminated bamboo lumber under tension parallel to grain were obtained. The tensile failure of side press-laminated bamboo lumber was a brittle fracture, and the typical failure mode can be classified into three types. The mean value for tensile strength was 127.18 MPa when there was no bamboo node, while the mean value was 89.99–107.37 MPa when there were one to three bamboo nodes. The number of bamboo nodes would significantly affect the tensile properties parallel to grain of side press-laminated bamboo lumber, whereas the position of bamboo nodes has an insubstantial impact. Comparisons with other research results were also carried out. A series of formulas were proposed based on the test results to reflect how the node influenced the mechanical properties of side press LBL under tensile conditions.

✉ Haitao Li
lhaitao1982@126.com

¹ College of Civil Engineering, Nanjing Forestry University, Nanjing 210037, China

² Joint International Research Laboratory of Bio-composite Building Materials and Structures, Nanjing Forestry University, Nanjing 210037, China

³ Ganzhou Sentai Bamboo Company LTD, Ganzhou 341001, China

⁴ University College London, London WC1E 6BT, UK

⁵ University of Naples Federico II, Via Claudio 21, 80133 Naples, Italy

Introduction

There are 78 genera divided into about 1500 species of bamboo all over the world, and the area of bamboo forests is about 20 million square hectares (Xu et al. 2007; Khalil et al. 2012). Bamboo tends to grow in a “belt” running through tropical, subtropical, and temperate climates around the globe, and up to 3500 m altitude (Kaminsky et al. 2016), of which 65% are grown in Asia (Paridah 2013). Compared with wood, the elasticity and strength of bamboo are higher (Chung and Yu 2002; Chen et al. 2006; Awalluddin et al. 2017). Bamboo has some other advantages over wood, such as a short growth cycle and high cleavability. In addition, the energy required to obtain bamboo, by volume, is much smaller than for steel, and the specific resistance, which is the material tensile strength divided by the material density, of bamboo can be six times higher than the steel one (Ghavami 1995, 2005).

Traditional bamboo structure buildings mainly use raw bamboo materials as basic components (Li et al. 2016a; Huang et al. 2016; Zhou et al. 2019; Fei et al. 2019). Due to the inherent disadvantages of raw bamboo such as small diameter, large variations in the geometric size, and mechanical properties, the raw bamboo components cannot meet the physical and mechanical properties requirements of modern building structures and component size, which has promoted the development of bamboo engineering products, such as bamboo scrimber and laminated bamboo lumber (LBL), compensating for the shortcomings of original bamboo material (Mahdavi et al. 2012; Verma and Chariar 2013; Correal et al. 2014; Sharma et al. 2015; Li et al. 2016b; Wei et al. 2017; Yu et al. 2017; Zhong et al. 2017; Lv et al. 2019; Shen et al. 2019; Chen et al. 2020; Sun et al. 2020). LBL is processed from fast-growing, short-cycle bamboo into fixed-width and fixed-thick bamboo strips, which are dried to achieve a moisture content of 8% to 12%, and then the bamboo strips are glued in the same direction to an arbitrary length and cross section through an adhesive (see Fig. 1a). As a bamboo engineering product, LBL can also achieve the natural aesthetic texture and fibrous property of bamboo. Many scholars have conducted experimental research on LBL and the basic properties of LBL have been tested. The results show that the strength and stiffness of LBL are equivalent to that of wood and can replace structural wood. Compared with traditional building materials such as concrete and steel, LBL has a good strength-to-weight ratio, which proves the feasibility of it as a structural material (Mahdavi et al. 2011; Sharma et al. 2016; Khoshbakht et al. 2017). Besides, LBL has proven to be an anisotropic material like wood by studying its elastic modulus and Poisson’s ratio (Takeuchi et al. 2015, 2018; Yang et al. 2020). There are many studies on LBL beams, slabs, and columns as well (Nugroho and Ando 2000, 2001; Sinha et al. 2014; Li et al. 2015a, b, c).

However, the existence of bamboo nodes makes the mechanical performance of bamboo more complicated compared to steel and other materials (Hamdan 2004; Anwar et al. 2005a, b; Razak et al. 2013). The node of bamboo culm consists of a sheath scar, nodal ridge, diaphragm, and internode between the nodal ridge and sheath scar (Liese 1998). The study of bamboo with its node present is very

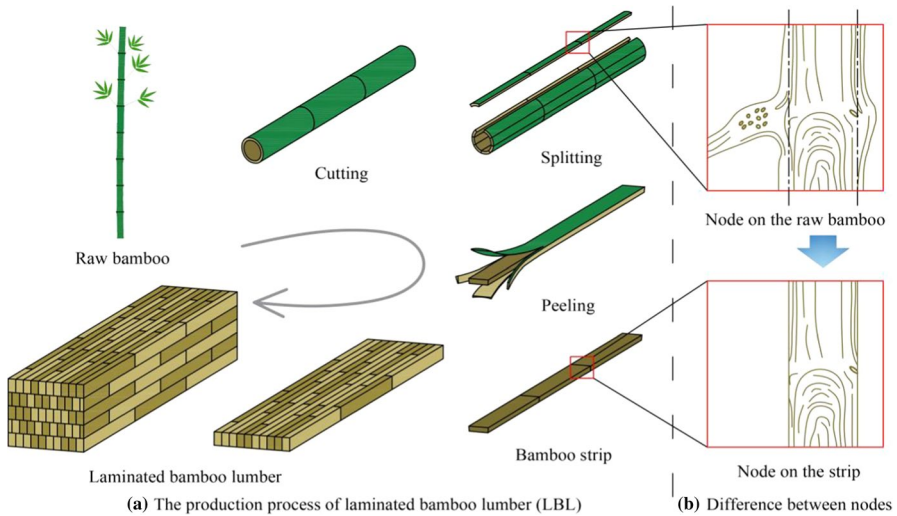


Fig. 1 Laminated bamboo lumber (LBL)

important to determine the influence of this portion on the properties of the bamboo (Sekhar and Bhartari 1960). The reason for it is that the existence of bamboo nodes reduces the uniformity, elasticity, and strength of bamboo (Hamdan et al. 2009). Although the results could be quite contrary by different researches with respect to the effect of a node on the bending, compression, and shear properties of bamboo, the negative effect upon shear properties is definite (Zeng et al. 1992; Shao et al. 2010). Furthermore, the internodal elastic modulus has been tested to be higher than the nodal parts (Nordahlia et al. 2011). Nonetheless, most of the existing studies upon bamboo nodes focus on the raw bamboo, and there is still a lack of researches on the nodes in LBL. Tests on several properties of LBL with or without nodes were carried out and demonstrated that nodes could significantly affect the thickness swelling, bending, and compression strength of LBL (Sulasatiningsih et al. 2013; Anokye et al. 2016). Nodes in the LBL are different from those in the raw bamboo because bamboo is processed during the production of LBL, as shown in Fig. 1b. Moreover, since LBL is composed of several bamboo strips, the distribution of nodes in LBL is random and many possible orderings may exist. Hence, LBLs were used to test and analyze the tensile properties parallel to grain of LBL under different conditions of nodes in this paper, providing a scientific basis for the development of LBL in civil engineering.

Experimental

Materials

The test material was side press LBL (*Phyllostachys edulis*) produced by Sentai Bamboo and Wood Co., Ltd., Jiangxi Province in China. With resorcinol as



Fig. 2 Node distribution of an LBL column

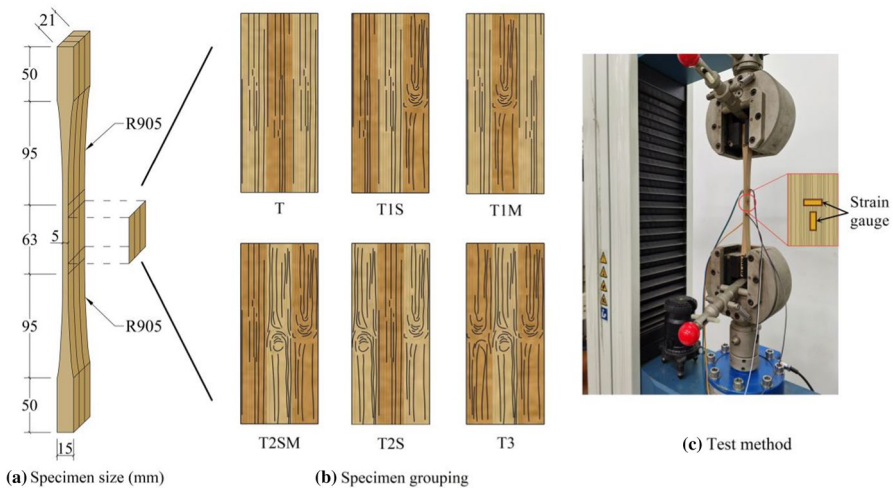


Fig. 3 Tensile specimen and test method

adhesive, laminated bamboo was made of three bamboo strips ($7 \times 21 \times 2000$ mm) glued together by hot pressing for about 15 min under the condition of main pressure of 9 MPa, side pressure of 6.5 MPa, and temperature of 157 °C, as shown in Fig. 1. The laminated bamboo lumber consists of many nodes. To analyze the tensile properties, the LBL was divided into several parts along the grain. Figure 2 shows an LBL column and the node distribution of it. Thus, a traditional dog bone specimen comprising three laminas was designed in accordance with the American

standard ASTM D143-94 and the Chinese national standard GB1927-1943-91. The dimensions are shown in Fig. 3a. The laminae of the specimen were cut from the bamboo strips with a thickness of 7 mm, which are typically used for the manufacture of LBL products. All sides of the specimen must be flat, and the four sides were perpendicular to each other. In addition, each end face must be smooth and flat, and perpendicular to the axis of the test specimen. Specimens not meeting the standard need to be polished again. The specimens were divided into six groups based on the differences in the position of the bamboo nodes, 30 replicates per group. Figure 3b schematically shows the positions of bamboo nodes in specimens of each group. Among them are T: without node, T1S: with one node, on one side strip, T1M: with one node, on the middle strip, T2SM: with two nodes, on one side and middle strips, T2S: with two nodes, on the strips both sides, T3: with three nodes on all three strips. The aim of this study is to find out the most unfavorable tensile position of the elements in engineering structures and analyze it. A series of aligned nodes is the most unfavorable position in an LBL structure. Therefore, the nodes on the specimen are aligned in the same line.

Methods

During the test, an electronic universal testing machine was used to apply a tensile force to the specimen in a continuous and uniform loading direction until the specimen lost its bearing capacity and was damaged (see Fig. 3c).

The main steps of the tensile test were as follows:

- a. Horizontal and vertical strain gauges were attached at the middle of the wide surface of the specimen, as shown in Fig. 3c, and the strain gauges were connected to a TDS-530 data logger. The size of the strain gauge-sensitive grid was 3 mm × 2 mm, the resistance was 120 Ω, and the adhesive used for attachment was instantaneous drying glue 502.
- b. The specimen was installed vertically in the claws of the testing machine, the wide surface of the specimen was in contact with the claw, and the position of the specimen was adjusted to ensure that the axis of the specimen was pulled.
- c. The test was loaded at a uniform speed of 1.5 mm/min.
- d. If the failure was not in the valid part of the specimen, the test results should be discarded.

Results and discussion

Failure phenomena

When the limit load was approached, a slight sound would appear, followed by continuous sounds. After that, the specimen fractured brittlely and a great cracking sound was emitted. The final failure mode can be classified into three types. The fracture of 77 specimens was relatively smooth, and cracks in the direction of the

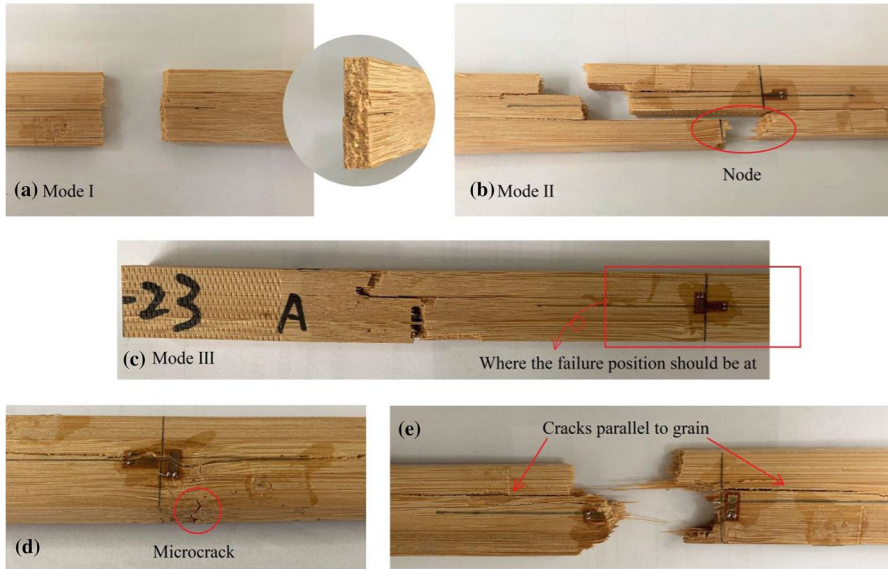


Fig. 4 Typical failure modes and fracture phenomena

fiber were basically absent. As shown in Fig. 4a, it was Mode I. Mode II was that the fracture of the specimen was not uniform, and there were cracks in the direction of the fiber. As shown in Fig. 4b, there were 87 specimens in this failure mode. Failure of some specimens did not occur in the ideal area, as illustrated in Fig. 4c, which was Mode III. This failure mode occurred in every group except for Group T3, with a total of 16 specimens. The results of such specimens were invalid. The number of specimens of different failure modes in each group is tabulated in Table 1.

Failure phenomena of Group T

When there was a slight sound, a small crack was generated along the fiber direction, and continuous sounds were issued. The crack rapidly propagated, causing a

Table 1 Summarized typical failure modes

Group	Mode I	Mode II	Mode III	Total
T	16 (53)	7 (23)	7	30
T1S	0	24 (80)	6	30
T1M	13 (43)	16 (53)	1	30
T2SM	13 (43)	16 (53)	1	30
T2S	17 (57)	12 (40)	1	30
T3	18 (60)	12 (40)	0	30
Total	77 (43)	87 (48)	16	180

Values in brackets are proportions of this mode (%)

rapid fracture and a large cracking sound. The final failure mode of 16 specimens was Mode I, accounting for 53% of the total specimens of the group. There were seven specimens each for Mode II and Mode III, accounting for 23%. The Mode III was most likely to occur in this group among all six groups, one reason may be that there was no node on the laminae which could be Achilles' heel to the specimen.

Failure phenomena of Group T1S

Microcracks were generated along with the fiber when the limit load was approached. After that, some of the specimens were broken suddenly, the others were fractured at the node first. The final failure of 6 specimens was Mode III, which accounted for 20%. The rest were Mode II, a total of 24 specimens, accounting for 80%. Due to the asymmetrically distributed node, the crack was uneven.

Failure phenomena of Group T1M

Specimens of Group T1M were abruptly broken, and cracks quickly propagated and made a loud cracking noise. Final failure modes: 13 specimens were Mode I (43% of all), 16 specimens were Mode II (53% of all), and 1 specimen was Mode III.

Failure phenomena of Group T2SM

At the beginning of the test, there was a slight noise, which caused microcracks (Fig. 4d) along with the fiber. In the later stage, 13 specimens were broken suddenly, and this type of fracture did not have parallel-to-grain cracks (Mode I, 43%). 16 specimens' fracture arose at the node on the side, then extended to the middle strip, finally went through the whole specimen, along with glue layer cracks developing (Mode II, 53%); in addition, there was a specimen that was Mode III.

Failure phenomena of Group T2S

A total of 17 specimens were suddenly fractured. The final fracture was symmetrically through the nodes on both sides (Mode I, 57%). Twelve specimens fractured at the node on one side laminae first, and then the whole specimen broke. This type of final failure generally fractured at the node on one side and fractured at the internode on the other side (Mode II, 40%). This group also has a Mode III specimen.

Failure phenomena of Group T3

Specimens of Group T3 all broke suddenly. The final failure mode was classified into two types: the fracture passed through 3 nodes, which was Mode I, 18 specimens, accounting for 60% of the total; the fracture only passed through 1 or 2 node(s), Mode II, 12 specimens, accounting for 40% of the total.

Failure phenomena analysis

From the results of the tests, it can be concluded that the specimens always broke at the natural defects of bamboo laminae, i.e., bamboo nodes, initially. For the specimens with nodes symmetrically distributed like those in Group T1M and T2S, the failure crack tended to be a flush cut edge, compared with those in Group T1S and T2SM, respectively. That is because the fracture of unsymmetrical nodes can lead to an eccentric tension of the specimen and the specimen being torn along the laminate surface (Fig. 4b). As the number of nodes increases, the fracture was more likely to occur at the node trimly, which demonstrated that the node is the weak link when the specimen is pulled.

However, the failure mode of the specimens in the same group seemed to be random. Although the fracture would go through the node definitely, the failure position of the laminae without node was uncertain.

Analysis of results

Load–displacement behaviors

The load–displacement curves of six groups of specimens are summarized in Fig. 5. At the beginning of the loading process, all the specimens went through the elastic stage, in which the stiffness of each group of specimens was relatively stable, and then entered the elastic–plastic stage with a gradual reduction in stiffness. After that, the load–displacement curves dropped rapidly, which showed that the specimen was broken. However, some of the curves rose again to a certain degree, which did not exceed the previous peak, illustrating that the specimen has undergone secondary damage. Compared to the ones in Group T, T1M and T3, the specimens of Group T1S, T2SM, and T2S were more prone to break strip by strip according to the curves, which was consistent with the experimental results.

Stress–strain behaviors

Figure 6 plots the stress–strain curves and stress–strain models for the test specimens. It can be seen from the curves that nonlinear behavior existed in the final loading stage for the specimens. The straight lines are chosen to show the stress/strain behaviors from a design perspective which could make the analysis easier with a high accuracy. However, the straight lines could not measure the true Young's modulus. Regardless of the existence of bamboo nodes, the model can be expressed as Eq. (1):

$$\sigma = E\varepsilon \quad (1)$$

where σ is the tensile stress of side press LBL, E is the elastic modulus, ε is the tensile strain.

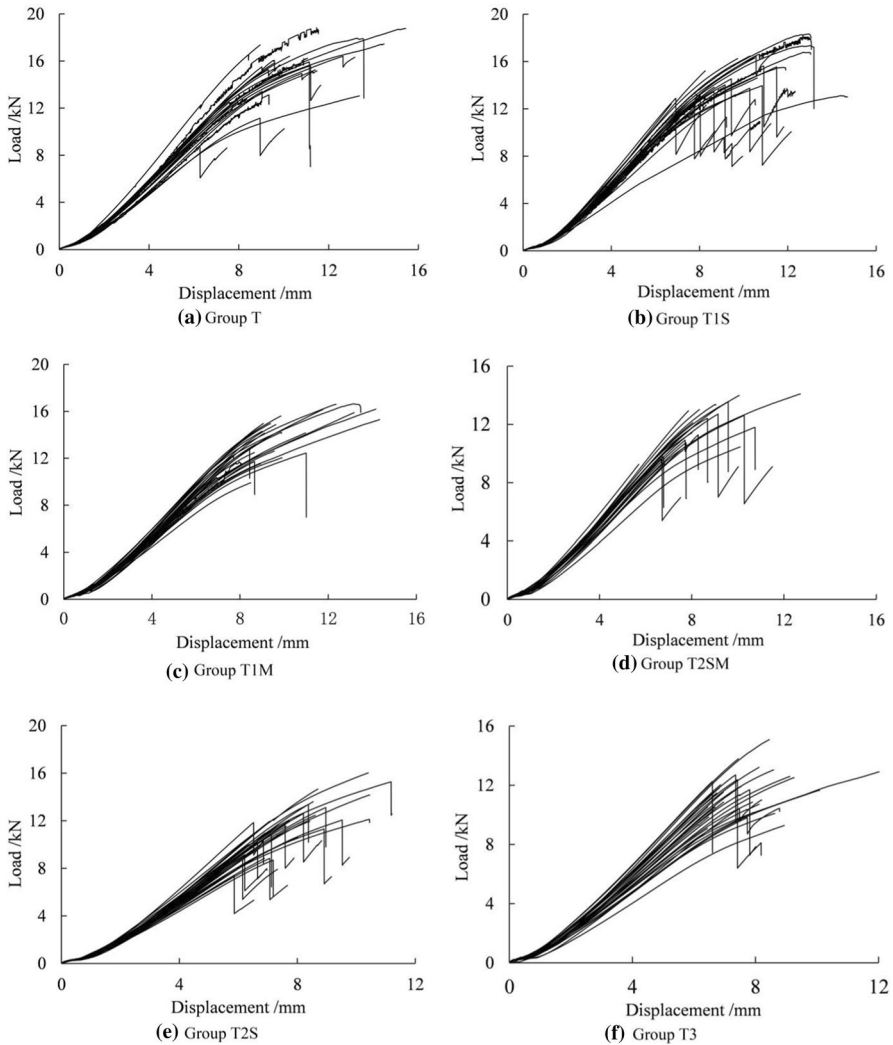


Fig. 5 Load–displacement curves

The stress–strain curve of the specimen in Fig. 6 was a straight line, and there was no evident yield platform, indicating that the tensile failure of side press LBL was brittle. As the number of nodes increased, the degree of dispersion of the curve in each group also increased, which indicated that the existence of nodes makes the elastic modulus of the specimens tend to be highly variable.

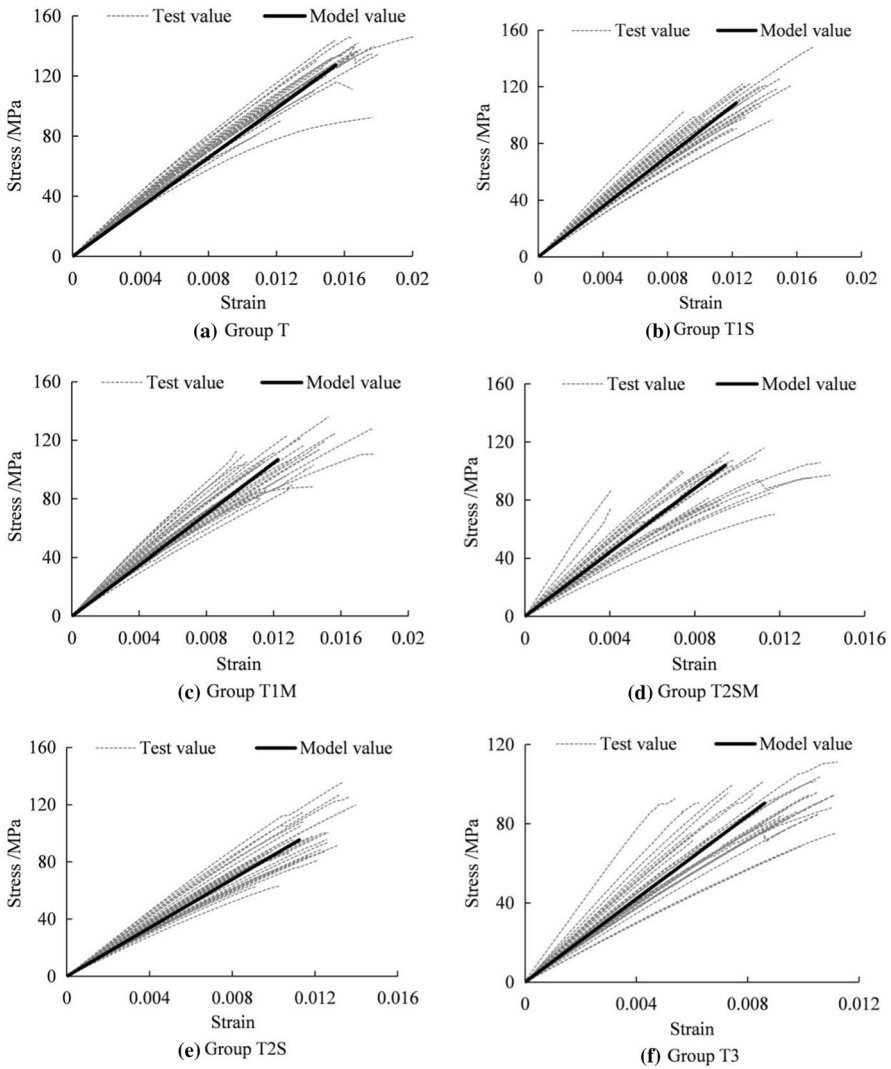


Fig. 6 Stress–strain curves and stress–strain models

Data analysis

The final calculation results for ultimate load F_u , tensile strength f_t , elastic modulus E , Poisson’s ratio μ , vertical ultimate strain $\epsilon_{u,V}$, and horizontal ultimate strain $\epsilon_{u,H}$ for group specimens are tabulated in Table 2.

Analysis of the test data shows that the mean value for the tensile strength of one-node specimens was 16% lower than that of the non-node specimens. For two-node and three-node specimens, the reduction was 24% and 29%, respectively. As shown in Fig. 7, the difference between the mean value for the tensile strength of the

Table 2 Tensile properties of side press LBL (with and without node) and the results of ANOVA

Group		T	T1S	T1M	T2SM	T2S	T3	F values	P values
F_u (kN)	Mean	15.38	14.85	13.68	11.6	11.63	11.55	19.194**	.000
	SDV	2.43	1.77	1.86	1.336	2.04	1.42		
	COV	15.81%	11.95%	13.62%	11.52%	17.56%	12.33%		
	CHV	11.38	11.93	10.61	9.33	8.27	9.21		
f_t (MPa)	Mean	127.18	107.37	106.57	96.949	95.12	89.99	17.837**	.000
	SDV	17.77	14.98	13.29	11.322	18.68	9.77		
	COV	13.97%	13.95%	12.47%	11.67%	19.64%	10.85%		
	CHV	97.95	82.73	84.71	77.73	64.39	73.93		
E (MPa)	Mean	8219	8870	8756	10,624	8480	10,503	17.149**	.000
	SDV	719	1067	1260	1374	1119	2448		
	COV	8.75%	12.03%	14.39%	12.93%	13.19%	23.31%		
	CHV	7036	7115	6683	8090	6640	6476		
μ	Mean	0.235	0.236	0.228	0.282	0.277	0.336	7.686**	.000
	SDV	0.020	0.060	0.058	0.085	0.073	0.138		
	COV	8.51%	25.42%	25.44%	30.14%	26.35%	41.07%		
	CHV	0.202	0.137	0.133	0.138	0.157	0.109		
$\epsilon_{u,V}$ ($\mu\epsilon$)	Mean	19,380	13,390	12,330	9430	12,033	9269	30.354**	.000
	SDV	3944	1703	2275	2512	1732	1650		
	COV	20.35%	12.72%	18.45%	26.64%	14.39%	17.80%		
	CHV	12,892	10,588	8588	5162	9185	6555		
$\epsilon_{u,H}$ ($\mu\epsilon$)	Mean	3710	3140	2860	2580	3263	2932	5.059**	.000
	SDV	740	983	635	1129	1198	994		
	COV	19.95%	31.31%	22.20%	43.76%	36.71%	33.90%		
	CHV	2492	1523	1816	662	1293	1297		

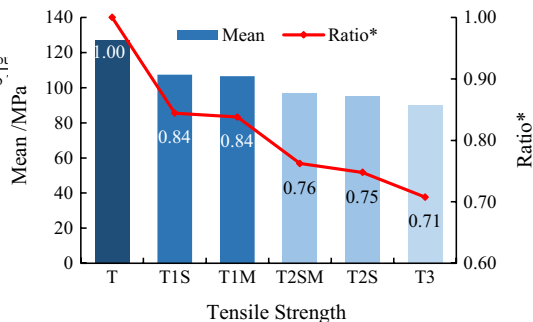
SDV means the standard deviation, COV means the coefficient of variation, CHV means characteristic value, calculated on the basis that 95% of samples exceed the characteristic value, ns Not significant, $P > 0.05$

*Significant at 95%

**Significant up to 95%

Fig. 7 Reduction in tensile strength,

* Ratio = $\frac{\text{the mean value for tensile strength of this group}}{\text{the mean value for tensile strength of Group T}}$



specimens with the same quantity of nodes seemed to be minimal, though the position of the node was different. As for elastic modulus, the node did not have a distinct effect on this value. Mean values for the elastic modulus of other groups were basically between 8000 and 9 000 MPa except that values of Group T2SM and T3 exceeded 10 000 MPa. As the nodes increased, the vertical and horizontal ultimate strains decreased, but the vertical one decreased faster, so the Poisson's ratio tended to increase. Besides, it is worth noting that for specimens with the same quantity of nodes, the ultimate strain varied greatly due to different positions of nodes. For example, the average vertical ultimate strain of the Group T2SM was 9 790, and the value of the Group T2S was 12 033. The position of the strain gauge might be the reason for it. The strain gauges of Group T1S and T2S were stuck at the internode, whereas Group T1M and T2SM were at the node. It can be inferred that the strain at the node was less than the internode at the same stress. In summary, the number of nodes can substantially reduce the tensile properties of LBL, while the position of the node makes a subtle difference.

Due to the huge difference among different bamboo individuals, the tensile properties of the specimens tend to be highly variable. As a bio-based composite, the properties of laminated bamboo are affected by the bamboo's natural properties. Although the number of nodes is the same in a group, the shape, the volume, and the consequent mechanical properties of each node are different, leading to a large deviation among each sample.

As the position of bamboo nodes has an insubstantial impact, the following analysis will focus on the fraction of node area. The scatter diagrams of tensile strength, elastic modulus, Poisson's ratio, vertical and horizontal ultimate strain are plotted in Figs. 8 and 9. The tensile strength and the fraction of node area can be described by Eq. (2):

$$f_t = (0.253x^2 - 0.542x + 1)\overline{f_{t,0}} \quad (2)$$

where f_t is the tensile strength, x is the fraction of node area, and $\overline{f_{t,0}}$ is the mean value for the tensile strength of Group T. Figure 8a shows that the tensile strength

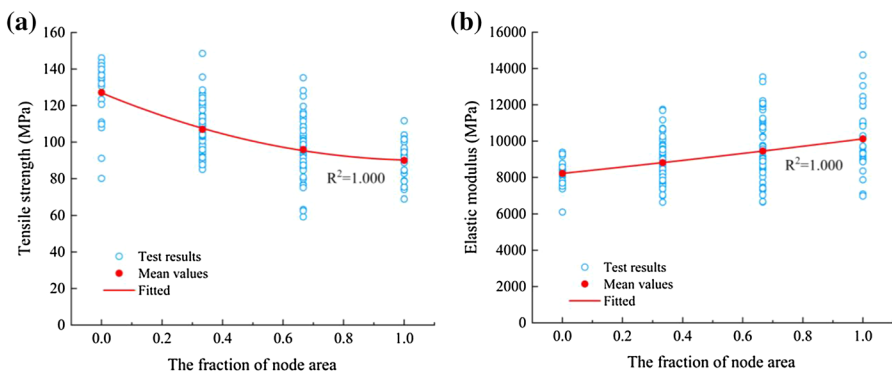


Fig. 8 Comparison of **a** tensile strength and **b** elastic modulus

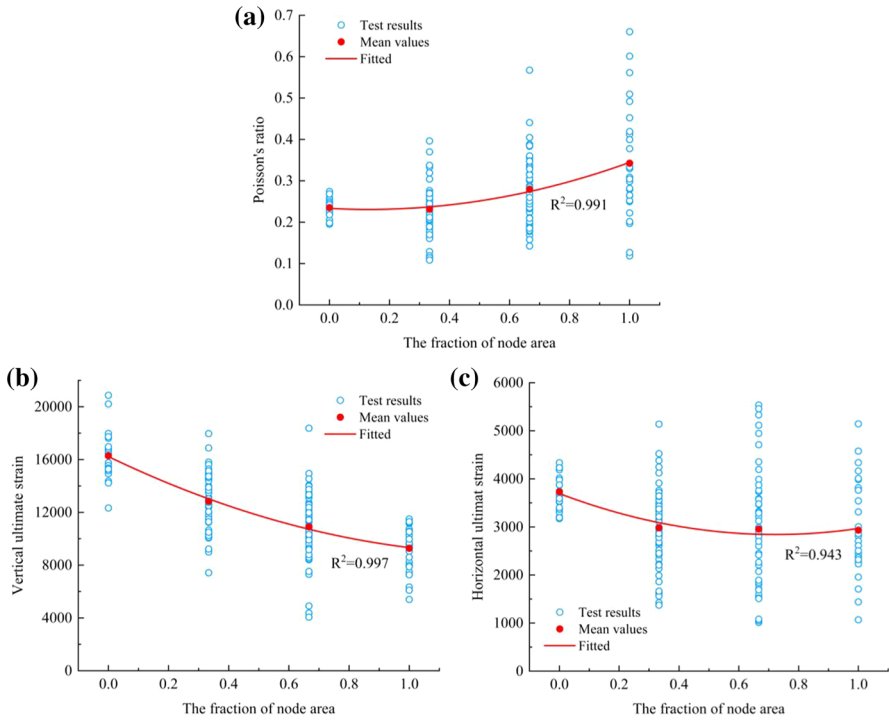


Fig. 9 Comparison of **a** Poisson's ratio, **b** vertical ultimate strain and **c** horizontal ultimate strain

decreased along with increasing fraction of the node area. When the fraction was 1, the degree of dispersion was the smallest, and the degree of dispersion was larger when the fraction was between 0 and 1. As discussed above, the initial fracture of the specimen occurred mostly in the nodal area. The tensile strength for the specimen was the load level of the first failure, which illustrated that the tensile strength of a specimen was determined by the weakest node on it. When the fraction of the node area was 1, the tensile strength was decided by the weakest one of the three nodes, which varied inconsiderably. However, if a specimen had only one node, the tensile strength was controlled by the only node, leading to a large degree of variation in tensile strength.

The elastic modulus and the fraction of node area can be described by Eq. (3):

$$E=(0.021x^2 + 0.210x + 1)\overline{E_0} \tag{3}$$

where E is the elastic modulus, x is the fraction of node area, and $\overline{E_0}$ is the mean value for the elastic modulus of Group T. Figure 8b shows that the elastic modulus increased along with the increasing fraction of the node area, and the degree of dispersion increased as the fraction of node area increased.

From Fig. 9, it can be seen that the vertical ultimate strain of the specimen decreased rapidly with the increase in the fraction, but the horizontal ultimate strain decreased slowly, so the Poisson's ratio showed an upward trend. The degree of

dispersion of the horizontal ultimate strain and Poisson's ratio increased with the increase in fraction, as well. As shown in Figs. 8 and 9, the degree of variation in tensile strength and vertical ultimate strain tended to decrease when the fraction of node increased while the degree tended to increase for elastic modulus, Poisson's ratio and horizontal ultimate strain.

The relationship between Poisson's ratio, the vertical ultimate strain, the horizontal ultimate strain and the fraction of node area can be described by Eqs. (4), (5), and (6):

$$\mu = 0.15x^2 - 0.039x + 0.233 \quad (4)$$

$$\varepsilon_{u,v} = 4071x^2 - 10971x + 16229 \quad (5)$$

$$\varepsilon_{u,H} = 1633x^2 - 2361x + 3695 \quad (6)$$

where μ is Poisson's ratio, $\varepsilon_{u,v}$ is the vertical ultimate strain ($\mu\varepsilon$), $\varepsilon_{u,H}$ is the horizontal ultimate strain ($\mu\varepsilon$), and x is the fraction of node area.

It is worth noting that the results are not limited to these particular specimens. They can also be applied to other LBL products with different dimensions or different numbers of layers.

Figure 10 shows the difference in strain between node and internode. When there was a node on the middle strip, the degree of dispersion of the ultimate strain and Poisson's ratio was greater because the strain gauge was stuck at the node.

The effects of the bamboo node on the tensile mechanical properties parallel to grain of LBL can be explained by the biological structure of bamboo internode and node at the micro-level. Compared with node, fibers in the internode are longer, parallel to each other and oriented uniformly (Sulthoni 1989; Liese 1980), which provides better resistance to tensile load for bamboo. Fibers in the node are also said to be short, forked and intersecting. Furthermore, the tensile strength of the vascular bundles is much higher than that of other tissues or the whole bamboo structure. The vascular bundles in the node are larger and longer than the internode (Nordahlia et al. 2011), and the distribution is disordered. The main vascular bundles in nodes are swollen, branching vascular anastomoses develop intensively, and many small vascular bundles turn horizontally and twist repeatedly (Sulthoni 1989; Liese 1980; Yulong and Liese 1997). Due to the swelling of the tissue at the node, the density of the node decreases slightly. These make the node a weak point in the tensile process of bamboo, which explains why most of the specimens broke at the nodes.

A comparison between the results of this test and similar tests is shown in Fig. 11. The performances of planed and intact (unplaned) bamboo nodes are quite different (Shao et al. 2010), so all the following comparative specimens of similar studies have flat surfaces for bamboo strips. Among them, the data of "with node" for LBL is the mean value for tensile strength of Group T3, and Glu-Bam (Wang et al. 2015) is the glued bamboo using *Phyllostachys edulis* as raw material. As can be seen from Fig. 11, all the tensile strength values for the specimens with nodes are smaller than the values for the specimens without nodes.

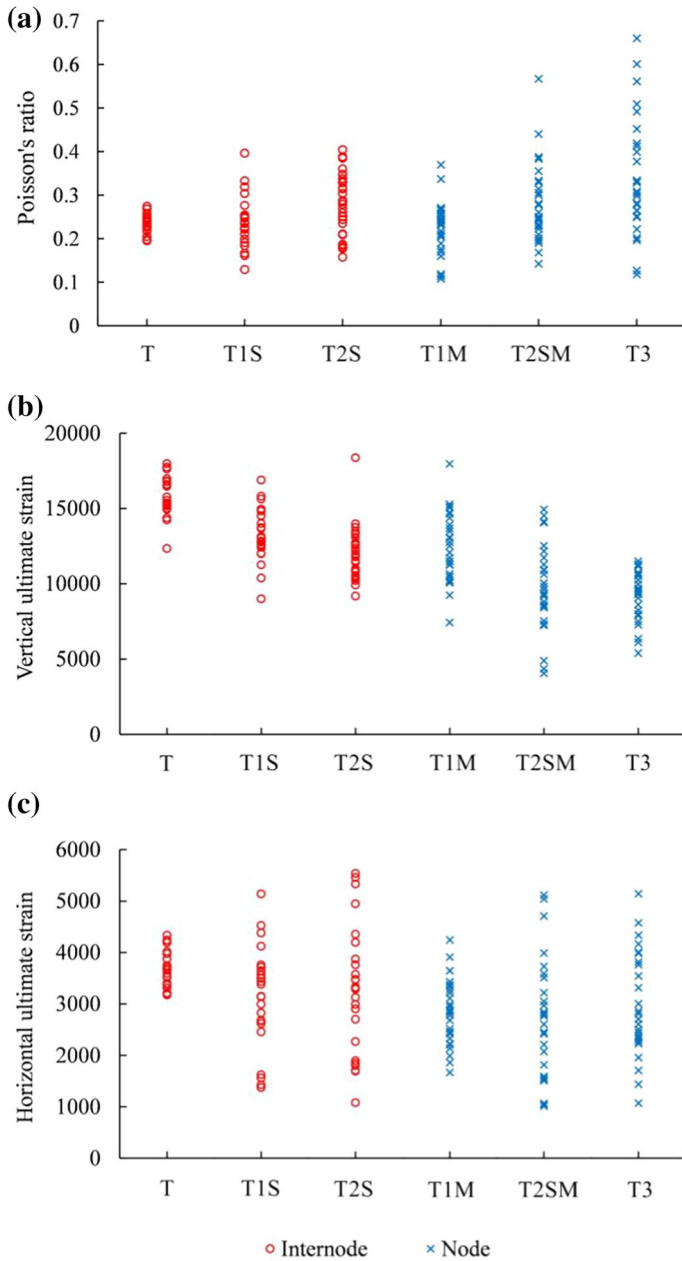


Fig. 10 Difference in strain between node and internode: **a** Poisson's ratio, **b** vertical ultimate strain and **c** horizontal ultimate strain

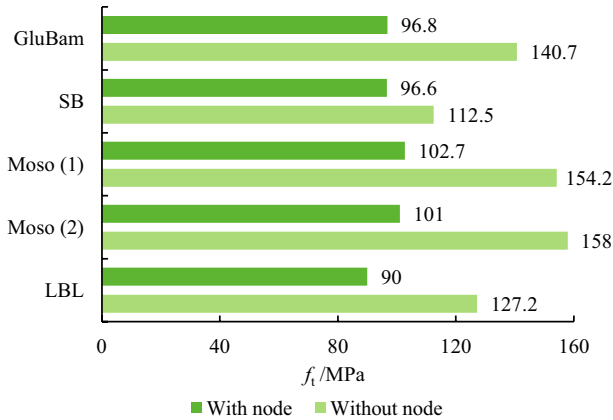


Fig. 11 Comparison with similar tensile test results. GluBam: Wang et al. (2015); SB: Semantan bamboo, Bahari et al. (2010); Moso (1): Shao et al. (2010); Moso (2): Taylor et al. (2015); LBL: present study

Table 3 Comparison with several kinds of wood and bamboo

	ρ (g cm ⁻³)	f_t (MPa)
Larix gmelini ^a	0.555–0.625	91.7
Sitka spruce ^b	0.383	59
Douglas-fir LVL ^c	0.52	49
Raw bamboo ^d	0.666	153
Raw bamboo ^e	About 0.7–0.95	148.9–229.4
GluBam ^f	0.7	83
Bamboo scrimber ^g	1.254	156.2
LBL (without node) ^h	0.734	127.18
LBL (with node) ^h	0.734	89.99–107.37

ρ is density

^aLarix gmelini: Zhou et al. (2016)

^bSitka spruce: Lavers (2002), Kretschmann (2010)

^cDouglas-fir LVL: Kretschmann et al. (1993), Clouston et al. (1998)

^dRaw bamboo *Phyllostachys pubescens*: DeVos (2010)

^eRaw bamboo *Phyllostachys pubescens*: Molaria et al. (2020)

^fGluBam: Xiao et al. (2013); Xiao and Shan (2013)

^gBamboo scrimber: Li et al. (2020)

^hPresent study

The value for LBL with nodes decreases by 29.2% which is close to that for GluBam with the percentage of 31.2%. The percentage of strength loss for Moso (1) and Moso (2) are 33.4% and 36.1%, respectively, while the percentage for SB (Bahari et al. 2010) is 14.1% which is the smallest one among all test results in Fig. 11.

Table 3 shows the density and tensile strength of several types of wood and bamboo. It can be seen that the tensile strength of LBL is comparable to that of other bamboo engineering products and higher than that of wood.

Conclusion

To evaluate the influence of the bamboo node on the tensile properties of side press-laminated bamboo lumber (LBL), 180 specimens were tested and the results were analyzed. The following conclusions are drawn.

- (1) As a building material, LBL can well meet the physical and mechanical requirement of practical applications. LBL has a higher density than wood products but a lower one than other bamboo engineering products. However, the tensile strength of LBL is comparable to that of other bamboo products and is higher than that of wood products, especially the one without node. Besides, the decrease rate of strength due to nodes is also comparable to other bamboo products.
- (2) The tensile failure of side press LBL was a brittle fracture. The stress–strain model of side press LBL could be expressed linearly with or without node from the design point of view. The tensile strength of side press LBL without node was 127.18 MPa, and the tensile strength with nodes decreased by 16% to 29%. The tensile strength of the specimen with 3 nodes was 89.99 MPa. As the number of nodes increased, the degree of dispersion of the elastic modulus and Poisson's ratio of the specimen increased. Under the same stress, the strain at the node was less than the strain at the internode.
- (3) In an LBL structure, nodes are the most unfavorable position of the tensile component such as the soffit of a beam. Characteristic values with a guarantee rate of 95% for tensile properties were obtained, which can be used as the lowest criterion in practical applications.
- (4) The effect of the position of the node on the tensile properties was not prominent. The negative effect of the node on the tensile properties of side press LBL is due to the difference in biological structure between nodes and internodes. The relationship between tensile strength, elastic modulus, Poisson's ratio, ultimate strain and the fraction of node area was proposed.
- (5) Comparisons with other research results were carried out. The node could influence the tensile strength obviously. The percentage of strength loss for LBL is 29.2% which is smaller but close to the values for GluBam, Moso (1) and Moso (2) with the percentage of 31.2%, 33.4% and 36.1%, respectively. While the percentage of strength loss for SB (Bahari et al. 2010) is the smallest one among all test results.

Acknowledgements The research work presented in this paper is supported by the National Natural Science Foundation of China (No. 51878354 & 51308301), the Natural Science Foundation of Jiangsu Province (No. BK20181402 & BK20130978), Six talent peak high-level projects of Jiang-su Province

(No. JZ-029), and a Project Funded by the Priority Academic Program Development of Jiangsu Higher Education Institutions. Any research results expressed in this paper are those of the writer(s) and do not necessarily reflect the views of the foundations. The writers gratefully acknowledge Ke Zhou, Hang Li, Xiaoyan Zheng, Shaoyun Zhu, Liqing Liu, Dunben Sun, Jing Cao, Yanjun Liu and others from the Nanjing Forestry University for helping with the tests.

References

- Anokye R, Bakar ES, Ratnasingam J, Yong ACC, Bakar NN (2016) The effects of nodes and resin on the mechanical properties of laminated bamboo timber produced from *Gigantochloa scortechinii*. *Constr Build Mater* 105:285–290. <https://doi.org/10.1016/j.conbuildmat.2015.12.083>
- Anwar UMK, Paridah MT, Hamdan H, Latif MA, Zaidon A (2005a) Adhesion and bonding properties of Plybamboo manufactured from *Gigantochloa scortechinii*. *Am J Appl Sci (Special Issue)*: 53–58
- Anwar UMK, Zaidon A, Hamdan H, Tamizi MM (2005b) Physical and mechanical properties of *Gigantochloa scortechinii* bamboo splits and strips. *J Trop For Sci* 17(1):1–12
- Awalluddin D, Mohd AM, Osman M, Hussin M, Seung LH, Abdul SLN (2017) Mechanical properties of different bamboo species. *MATEC Web Conf* 138:01024. <https://doi.org/10.1051/mateconf/201713801024>
- Bahari SA, Ahmad M, Nordin K, Jamaludin MA (2010) Tensile Mechanics of Bamboo Strips. In: International conference on advancement of materials and nanotechnology 2007 (ICAMN 2007), vol 1217, pp 457–461. <https://doi.org/10.1063/1.3377866>
- Chen JM, Lin JG, Xu GQ, Wu LQ, Xu XF (2006) Present situation of utilization technology for bamboo resources and development counter measures for bamboo industry. *Subtrop Agric Res* 2(3):216–220
- Chen G, Yu YF, Li X, He B (2020) Mechanical behavior of laminated bamboo lumber for structural application: an experimental investigation. *Eur J Wood Prod* 78(1):53–63. <https://doi.org/10.1007/s00107-019-01486-9>
- Chung KF, Yu WK (2002) Mechanical properties of structural bamboo for bamboo scaffoldings. *Eng Struct* 24(4):429–442. [https://doi.org/10.1016/S0141-0296\(01\)00110-9](https://doi.org/10.1016/S0141-0296(01)00110-9)
- Clouston P, Lam F, Barret JD (1998) Incorporating size effects in the Tasi-Wu strength theory for Douglas-fir laminated veneer. *Wood Sci Technol* 32(3):215–226. <https://doi.org/10.1007/BF00704844>
- Correal JF, Echeverry JS, Ramírez F, Yamin LE (2014) Experimental evaluation of physical and mechanical properties of Glued Laminated *Guadua angustifolia* Kunth. *Constr Build Mater* 73:105–112. <https://doi.org/10.1016/j.conbuildmat.2014.09.056>
- DeVos V (2010) Bamboo for exterior joinery: a research in material properties and market perspectives. Dissertation, Larenstein University
- Fei B, Liu R, Liu X, Chen X, Zhang S (2019) A review of structure and characterization methods of bamboo pits. *J For Eng* 4(2):13–18. <https://doi.org/10.13360/j.issn.2096-1359.2019.02.002>
- Ghavami K (1995) Ultimate load behavior of bamboo reinforced lightweight concrete beams. *Cem Concr Compos* 17(4):281–288. [https://doi.org/10.1016/0958-9465\(95\)00018-8](https://doi.org/10.1016/0958-9465(95)00018-8)
- Ghavami K (2005) Bamboo as reinforcement in structural concrete elements. *Cem Concr Compos* 27(6):637–649. <https://doi.org/10.1016/j.cemconcomp.2004.06.002>
- Hamdan H (2004) Characterization of mechanical properties and behaviour of *Gigantochloa scortechinii* for structural application. Dissertation, University of Wales
- Hamdan H, Anwar UMK, Zaidon A, Tamizi MM (2009) Mechanical properties and failure behaviour of *Gigantochloa scortechinii*. *J Trop For Sci* 21(4):336–344
- Huang M, Zhang X, Yu W, Li W, Liu X, Zhang W (2016) Mechanical properties and structure characterization of bamboo softened by high temperature steam. *J For Eng* 1(4):64–68. <https://doi.org/10.13360/j.issn.2096-1359.2016.04.010>
- Kaminsky S, Lawrence A, Trujillo D (2016) Structural use of bamboo, part 1: introduction to bamboo. *Struct Eng* 94(8):40–43
- Khalil HPSA, Bhat IUH, Jawaid M, Zaidon A, Hermawan D, Hadi YS (2012) Bamboo fibre reinforced biocomposites: a review. *Mater Des* 42:353–368. <https://doi.org/10.1016/j.matdes.2012.06.015>
- Khoshbakht N, Clouston PL, Arwade SR, Schreyer AC (2017) Computational modeling of laminated veneer bamboo dowel connections. *J Mater Civ Eng* 30(2):04017285. [https://doi.org/10.1061/\(ASCE\)MT.1943-5533.0002135](https://doi.org/10.1061/(ASCE)MT.1943-5533.0002135)

- Kretschmann DE (2010) Mechanical properties of wood. In: Wood Handbook, General Technical Report FPLGTR-190. U.S. Department of Agriculture, Forest Service, Forest Products Laboratory, Madison, WI, pp 1–46
- Kretschmann DE, Moody RC, Pellerin RF, Bendtsen BA, Cahill JM (1993) Effect of various proportions of juvenile wood on laminated veneer lumber. Technical Report FPL-RP-521. U.S. Department of Agriculture, Forest Service, Forest Products Laboratory, Madison, WI
- Lavers GM (2002) The strength properties of timber, 3rd edn. Building Research Establishment (BRE), London
- Li HT, Su JW, Zhang QS, Chen G (2015a) Experimental study on mechanical performance of side pressure laminated bamboo beam. *J Build Struct* 36(3):121–126. <https://doi.org/10.14006/j.jzjxb.2015.03.015>
- Li HT, Su JW, Zhang QS, Deeks AJ, Hui D (2015b) Mechanical performance of laminated bamboo column under axial compression. *Compos Part B* 79:374–382. <https://doi.org/10.1016/j.compositesb.2015.04.027>
- Li Y, Xu B, Zhang Q, Jiang S (2016a) Present situation and the countermeasure analysis of bamboo timber processing industry in China. *J For Eng* 1(1):2–7. <https://doi.org/10.13360/j.jssn.2096-1359.2016.01.001>
- Li HT, Wu G, Zhang QS, Su JW (2016b) Mechanical evaluation for laminated bamboo lumber along two eccentric compression directions. *J Wood Sci* 62(6):503–517. <https://doi.org/10.1007/s10086-016-1584-1>
- Li Z, He MJ, Tao D, Li ML (2016c) Experimental buckling performance of scrimber composite columns under axial compression. *Compos Part B* 86:203–213. <https://doi.org/10.1016/j.compositesb.2015.10.023>
- Li HT, Zhang HZ, Qiu ZY, Su JW, Wei DD, Lorenzo R, Yuan CG, Liu HZ, Zhou CG (2020) Mechanical properties and stress strain relationship models for bamboo scrimber. *J Renew Mater* 8(1):13–27. <https://doi.org/10.32604/jrm.2020.09341>
- Liese W (1980) Anatomy of bamboo. In: Proceeding of a workshop, bamboo research in Asia. International Development Research Centre and the International Union of Forestry Research Organizations, pp 161–172
- Liese W (1998) The anatomy of bamboo culms. INBAR. Technical Report 18, Beijing, China
- Lv QF, Ding Y, Liu Y (2019) Study of the bond behaviour between basalt fibre-reinforced polymer bar/sheet and bamboo engineering materials. *Adv Struct Eng* 22(14):3121–3133. <https://doi.org/10.1177/1369433219858725>
- Mahdavi M, Clouston PL, Arwade SR (2011) Development of laminated bamboo lumber: review of processing, performance, and economical considerations. *J Mater Civ Eng* 23(7):1036–1042. [https://doi.org/10.1061/\(ASCE\)MT.1943-5533](https://doi.org/10.1061/(ASCE)MT.1943-5533)
- Mahdavi M, Clouston PL, Arwade SR (2012) A low-technology approach toward fabrication of laminated bamboo lumber. *Constr Build Mater* 29:257–262. <https://doi.org/10.1016/j.conbuildmat.2011.10.046>
- Molaria L, Mentrastib L, Fabianic M (2020) Mechanical characterization of five species of Italian bamboo. *Structures* 24:59–72. <https://doi.org/10.1016/j.istruc.2019.12.022>
- Nordahlia AS, Anwar UMK, Hamdan H, Latif MA, Mahanim SMA (2011) Anatomical, physical and strength properties of *Shizostachyum brachycladum* (Buluh lemang). *J Bamboo Rattan* 10(3&4):111–122
- Nugroho N, Ando N (2000) Development of structural composite products made from bamboo I: fundamental properties of bamboo zephyr board. *J Wood Sci* 46(1):68
- Nugroho N, Ando N (2001) Development of structural composite products made from bamboo II: fundamental properties of laminated bamboo lumber. *J Wood Sci* 47(3):237
- Paridah MT (2013) Bonding with natural fibres, 1st edn. Universiti Putra Malaysia Press, Serdang
- Razak W, Mustafa MT, Sukhairi M et al (2013) Anatomy and strength properties between tropical bamboo *Gigantochloa levis* and *G. scortechinii*. In: 2nd International conference on kenaf and applied fibres (ICKAF), pp 1–16
- Sekhar AC, Bhartari RK (1960) Studies on strength of bamboos: a note on its mechanical behaviour. *Indian For* 86:296–301
- Shao ZP, Zhou L, Liu YM, Wu ZM, Arnaud C (2010) Differences in structure and strength between internode and node sections of moso bamboo. *J Trop For Sci* 22:133–138. <https://doi.org/10.1007/s10310-009-0161-5>
- Sharma B, Gatóo A, Ramage MH (2015) Effect of processing methods on the mechanical properties of engineered bamboo. *Constr Build Mater* 83:95–101. <https://doi.org/10.1016/j.conbuildmat.2015.02.048>
- Sharma B, Bauer H, Schickhofer G, Ramage MH (2016) Mechanical characterisation of structural laminated bamboo. *P I Civil Eng Struct B* 170(4):250–264. <https://doi.org/10.1680/jstbu.16.00061>

- Shen YR, Huang DS, Chui YH, Dai C (2019) Fracture of parallel strand bamboo composite under mode I loading: DCB test investigation. *Adv Mater Sci Eng*. <https://doi.org/10.1155/2019/7657234>
- Sinha A, Way D, Mlasko S (2014) Structural performance of glued laminated bamboo beams. *J Struct Eng* 140(1):04013021-1-8. [https://doi.org/10.1061/\(ASCE\)ST.1943-541X.0000807](https://doi.org/10.1061/(ASCE)ST.1943-541X.0000807)
- Sulastiningsih IM, Ruhendi S, Massijaya MY, Darmawan IW, Santoso A (2013) Effects of nodes on the properties of laminated bamboo lumber. *Wood Res J* 4(1):19–24
- Sulthoni A (1989) Bamboo: physical properties, testing methods and means of preservation. In: Proceeding of a workshop on design and manufacture of bamboo and rattan furniture. Asia Pacific Forest Industry Development Group:4-1-4-13
- Sun XF, He MJ, Li Z (2020) Novel engineered wood and bamboo composites for structural applications: state-of-art of manufacturing technology and mechanical performance evaluation. *Constr Build Mater* 249:118751. <https://doi.org/10.1016/j.conbuildmat.2020.118751>
- Takeuchi CP, Estrada M, Linero DL (2015) The elastic modulus and Poisson's ratio of laminated bamboo *Guadua angustifolia*. *Key Eng Mater* 668:126–133. <https://doi.org/10.4028/www.scientific.net/KEM.668.126>
- Takeuchi CP, Estrada M, Linero DL (2018) Experimental and numerical modeling of shear behavior of laminated *Guadua* bamboo for different fiber directions. *Constr Build Mater* 177:23–32. <https://doi.org/10.1016/j.conbuildmat.2018.05.040>
- Taylor D, Kinane B, Sweeney C, Sweetnam D, O'Reilly P, Duan K (2015) The biomechanics of bamboo: investigating the role of the nodes. *Wood Sci Technol* 49:345–357. <https://doi.org/10.1007/s00226-014-0694-4>
- Verma CS, Chariar VM (2013) Stiffness and strength analysis of four layered laminate bamboo composite at macroscopic scale. *Compos Part B* 45(1):369–376. <https://doi.org/10.1016/j.compositesb.2012.07.048>
- Wang WJ, Zuo HL, Guo N, Han X (2015) The mechanical property tests for structural GluBam of the tensile strength parallel to grain. *Low Temp Arch Technol* 4:38–40. <https://doi.org/10.13905/j.cnki.dwjz.2015.04.014>
- Wei Y, Ji X, Duan M, Li G (2017) Flexural performance of bamboo scrimber beams strengthened with fiber-reinforced polymer. *Constr Build Mater* 142:66–82. <https://doi.org/10.1016/j.conbuildmat.2017.03.054>
- Xiao Y, Shan B (2013) *GluBam structures*. China Building Industry Press, Beijing
- Xiao Y, Yang RZ, Shan B (2013) Production, environmental impact and mechanical properties of glubam. *Constr Build Mater* 44(1):765–773. <https://doi.org/10.1016/j.conbuildmat.2013.03.087>
- Xu JM, Zhao RJ, Fei BH (2007) Research on properties and utilization of bamboo in China. *Wood Process Mach* 3:39–42. <https://doi.org/10.13594/j.cnki.mcjgix.2007.03.011>
- Yang D, Li HT, Xiong ZH, Mimendi L, Lorenzo R, Corbi I, Corbi O, Hong CK (2020) Mechanical properties of laminated bamboo under off-axis compression. *Compos Part A Appl S* 138:106042. <https://doi.org/10.1016/j.compositesa.2020.106042>
- Yu YL, Liu R, Huang YX, Meng FD, Yu WJ (2017) Preparation, physical, mechanical, and interfacial morphological properties of engineered bamboo scrimber. *Constr Build Mater* 157:1032–1039. <https://doi.org/10.1016/j.conbuildmat.2017.09.185>
- Yulong D, Liese W (1997) Anatomical investigations on the nodes of bamboo. *The bamboo*. The Linnean Society of London, London, pp 269–283
- Zeng QW, Li SH, Bao XR (1992) Effect of bamboo nodal on mechanical properties of bamboo wood. *Scientia Silvae Sinicae* 28(3):247–252
- Zhong Y, Wu GF, Ren HQ, Jiang ZH (2017) Bending properties evaluation of newly designed reinforced bamboo scrimber composite beams. *Constr Build Mater* 143:61–70. <https://doi.org/10.1016/j.conbuildmat.2017.03.052>
- Zhou JL, Feng X, Zhou XY (2016) Experimental research on mechanical properties of larch glulam. *J Cent South Univ T* 36(8):125–129. <https://doi.org/10.14067/j.cnki.1673-923x.2016.08.022>
- Zhou N, Zhang G, Huang D, Jiang S, Zhang Q (2019) Examination of dynamic characteristics of new bamboo structure by impact hammer test. *J For Eng* 4(2):54–60. <https://doi.org/10.13360/j.issn.2096-1359.2019.02.009>

Publisher's Note Springer Nature remains neutral with regard to jurisdictional claims in published maps and institutional affiliations.